Earth and Planetary Science Letters 317-318 (2012) 204–217

Contents lists available at SciVerse ScienceDirect

Earth and Planetary Science Letters

journal homepage: www.elsevier.com/locate/epsl

# Testing absolute plate reference frames and the implications for the generation of geodynamic mantle heterogeneity structure

G.E. Shephard [a,*], H.-P. Bunge [b], B.S.A. Schuberth [c], R.D. Müller [a], A.S. Talsma [a], C. Moder [b], T.C.W. Landgrebe [a]

[a] School of Geosciences, University of Sydney, Sydney, Australia
[b] Department of Earth and Environmental Sciences, University, Munich, Germany
[c] UMR GéoAzur, Univeristé de Nice, Valbonne, France

ARTICLE INFO

*Article history:*
Received 8 April 2011
Received in revised form 15 August 2011
Accepted 21 November 2011
Available online xxxx

Editor: L. Stixrude

*Keywords:*
absolute plate motion
subduction
plate tectonics
geodynamic modelling
true polar wander
hotspots

ABSTRACT

Absolute reference frames are a means of describing the motion of plates on the surface of the Earth over time, relative to a fixed point or "frame." Multiple models of absolute plate motion have been proposed for the Cretaceous–Tertiary period, however, estimating the robustness and limitations of each model remains a significant limitation for refining both regional and global models of plate motion as well as fully integrated and time dependent geodynamic models. Here, we use a novel approach to compare five models of absolute plate motion in terms of their consequences for forward modelled deep mantle structure since at least 140 Ma. We show that the use of hotspots, either fixed or moving, or palaeomagnetics, with or without corrections for true-polar wander, leads to significant differences in palaeo-plate velocities of over 10 cm/yr as well as differences in the location of palaeo-plate boundaries of up to 30° in longitude and latitude. Furthermore, we suggest that first order differences in forward predicted mantle structure between the models are due mostly to differences in palaeo-plate velocities, whereas variation in the location of plate boundaries may contribute to smaller wavelength offsets. We present a global comparison of the absolute reference frames in terms of mantle structure, which we have tomographically filtered to reflect the resolution of the seismic tomography model S20RTS. At very long wavelengths hotspot models best reproduce the mantle structure. However, when geometry and the match of smaller-scale subducted slab volumes are compared, a hybrid model based on moving hotspots after 100 Ma and palaeomagnetic data before (with no corrections for true-polar wander), best reproduces the overall mantle structure of slab burial grounds, even though no single model fits best at all mantle depths. We find also that the published subduction reference frame tested here results in a modelled mantle structure that agrees well with S20RTS for depths >2500 km, equivalent to subduction before the Cretaceous, but not for shallower depths. This indicates that a careful assimilation of hotspot, palaeomagnetic and seismic tomography data into future absolute plate motion models is required to derive a more robust subduction reference frame.



## 1. Introduction

Describing the motion of tectonic plates over geological time includes both relative motion and absolute motion. Much attention has been focused on refining relative plate motion models, mainly because they are better constrained by geophysical and geological observations than absolute plate motions. However, the use of a robust absolute reference frame is essential when plate motions are tied to the history of mantle convection. An absolute reference frame represents a means of describing the motion of plates on the surface of the Earth relative to a fixed reference frame, often the underlying mantle or Earth's spin axis. The problem with absolute plate motion models is that the data and methods used to create them do not necessarily result in models that are consistent with the history of subduction as interpreted in the structure of the deep mantle.

Models of absolute reference frames can be based on several lines of observations including hotspot tracks displaying age progression, and assuming either fixed or moving hotspots, as well as palaeomagnetically-based reference frames, with or without true polar wander corrections, subduction reference frames and hybrids of some or all the above. As a result, several absolute reference frames for Cretaceous–Tertiary plate tectonic reconstructions have been proposed. However, the use of such reference frames demands careful consideration in terms of the limitations of given sets of observations and the assumptions that are used to develop these absolute plate motion models, and in particular, their consequences for deep-mantle structure.

Alternative models of absolute reference frames imply a particular history of subduction zone locations through time, as well as an

* Corresponding author at: Madsen Building, School of Geosciences, University of Sydney, NSW, 2069, Australia. Tel.: +61 2 9351 8093 (office), +61 416598162 (mobile).
*E-mail address:* grace.shephard@sydney.edu.au (G.E. Shephard).

0012-821X/$ – see front matter 
doi:10.1016/j.epsl.2011.11.027

associated history of plate velocities. These surface dynamics impart effects on the location and timing of slab subduction and the evolution of mantle heterogeneity via the mixing of subducted material with the mantle. Differences between the locations of subduction margins through time and the locations of piles of subducted slabs can, in part, be linked to a poor absolute reference frame from which subduction zone locations through time are constrained (van der Meer et al., 2010).

Global geodynamic models are aimed at linking plate tectonics with mantle structure and require the construction of plate kinematic models that result in a subduction history compatible with the observed mantle structure. We examine the robustness of five absolute plate motion models, in a geodynamic context, through the observed distribution of slab material in the mantle (seismic tomography) versus that predicted by a forward geodynamic model. Surface kinematics are given by self-consistent plate-boundaries that follow the rules of plate tectonics and observational constraints as to the geometry of divergent and convergent plate boundaries, seafloor isochrons and data constraining the initiation or cessation of subduction and subduction polarity. By keeping all relative rotations and mantle convection parameters constant, we assess the fundamental differences that alternative absolute plate motion models impart on geodynamic models, and establish a framework for examining absolute plate motion in a mantle convection context.

## 2. Absolute reference frames

Some first-order constraints on absolute plate motion histories since the Mid-Cretaceous are given by hotspot tracks with clear age progressions (e.g. Müller et al., 1993; Norton, 1996), representing plate motions over relatively stable upwellings in the mantle, such as mantle plumes. Hotspots used for constraining absolute plate motion models may be regarded as fixed (Morgan, 1984; Wilson, 1963) or moving (e.g. Steinberger, 2000). The use of hotspot tracks in constraining plate motions for geodynamic modelling demands a consideration of mantle dynamics, especially upper mantle flow and the temporal effects on hotspot motion (Davies and Davies, 2009; Tarduno et al., 2009). However, numerical models considering plume deflection are themselves subject to considerable uncertainties. The absence of continuous hotspot trails prior to ~130 Ma, eliminates their use in well-constrained absolute plate motion models, and global reference frames for earlier times are usually based on palaeomagnetic data.

Palaeomagnetic data are obtained via the remnant magnetism of igneous or sedimentary rocks. However, they offer no longitudinal constraints due to Earth's magnetic dipole field axial symmetry. Furthermore, palaeomagnetic models are complicated by considerations of true polar wander (TPW) (Steinberger and Torsvik, 2010), meaning that the net motion caused by changing magnetic poles must be isolated. This requires computations of relative rotations and mean plate motion of all continents. The estimates of net motion are variable and can lead to different magnitudes of the correction applied, and therefore different models of TPW-corrected reference frames. TPW has been shown to be relatively small in the last 100 Myrs (Steinberger and Torsvik, 2008) even in studies of vigorous mantle circulation (Schaber et al., 2009) owing to the effect of a large lower mantle viscosity, and is therefore only applied to earlier times. A new breed of hybrid absolute reference models has recently emerged (Steinberger and Torsvik, 2008; Torsvik et al., 2008) using both hotspot and palaeomagnetic reference frames.

There has been previous work in comparing alternative absolute reference frames in terms of surface kinematics, such as net lithosphere rotation (Torsvik et al., 2010). However, the consequences for global deep mantle structure remain unknown. Here we compare five published absolute plate motion models (Table S1), including two hotspot models; a fixed hotspot model and a hybrid moving and fixed hotspot model, and three other hybrid models; a hybrid moving hotspot and palaeomagnetic model, a hybrid moving hotspot and TPW-corrected palaeomagnetic model, and a hybrid subduction reference frame.

### 2.1. Hybrid hotspot model

The "hybrid hotspot model" is based on moving African hotspots (located in the Indian and Atlantic oceans) from 100 Ma to present (O'Neill et al., 2005), and fixed hotspots (Müller et al., 1993) for older times. The generation of a reference frame based on the differential motion of individual hotspot tracks requires a consideration of backward-advected large-scale mantle flow based on seismic tomography, viscosity structure and plate motions, as well as the location of plume conduit contact with the lithosphere (Torsvik et al., 2010). Limitations of the O'Neill et al. (2005) method for moving hotspots include the linearity and reliability of age data along a hotspot track, neo-volcanism, and possible plume–ridge interaction (O'Neill et al., 2005; Torsvik et al., 2010).

### 2.2. Fixed hotspot model

This model is based on the geometry and radiometric age dates of volcanic chains with age progression from the Indian and Atlantic oceans, covering ages from ~132 Ma to present-day, combined with a relative plate motion model and assuming hotspot fixity (Müller et al., 1993). For consistency across models, imposed rotations for Africa have been extrapolated back to 140 Ma. Compared to Pacific hotspots, Indo-Atlantic hotspots are thought to have moved considerably less relative to each other. Prior to 80 Ma the rotations (including the Indian, Australian and Antarctic plates) are based only on the geometry and age progression of the New England seamount chain and the Walvis Ridge/Rio Grande Rise. Disagreements between hotspot and palaeomagnetic reference frames have been documented for India (Müller et al., 1994) and Australia (Idnurm, 1985), suggesting that the mantle underlying the Indian Ocean may not have provided a fixed reference frame. Palaeopoles for India from the Rajmahal Traps (Das et al., 1996; Rao and Rao, 1996) result in a palaeolatitude of the traps at their time of formation (~117 Ma) at 47°S (±400 km), whereas the Müller et al. (1993) model places them at 40°S(±400 km). A comparison of mid-Cretaceous (122–80 Ma) palaeo-latitudes of North America (NAM) and Africa from palaeomagnetic data with those from hotspot tracks (Van Fossen and Kent, 1992) provided evidence for an 11–13° discrepancy, indicating that Atlantic hotspots may have moved southwards between 100 and 130 Ma. However, others argue that this apparent southward movement was caused by TPW (Prévot et al., 2000).

### 2.3. Hybrid moving hotspot and palaeomagnetic model

This model uses moving Indo-African hotspots from 100 Ma to present (O'Neill et al., 2005) and a palaeomagnetic model (Torsvik et al., 2008) between 140 and 100 Ma. Herein, this model is referred to as the "hybrid palaeomagnetic model". In this model Africa is longitudinally fixed from 140 to 100 Ma, the rationale of which is based on the assumption that Africa has been surrounded by mid-ocean ridges since the breakup of Pangea (Torsvik et al., 2008).

### 2.4. Hybrid moving hotspot and TPW-corrected palaeomagnetic model

This model also uses the moving Indo-African hotspots (O'Neill et al., 2005) for times after 100 Ma and a TPW-corrected palaeomagnetic framework (Steinberger and Torsvik, 2008) for earlier times. This model also assumes zero longitudinal motion of Africa and will be referred to as the "hybrid TPW-corrected model".

### 2.5. Subduction reference model

We also include a recently published model which used a novel approach of correcting absolute plate motion based on the location of subducted slabs in the mantle, slab sinking rates and the location of surface subduction (van der Meer et al., 2010). This subduction reference model is based on the hybrid TPW-corrected model (O'Neill et al., 2005; Steinberger and Torsvik, 2008), but imposes a slab correction for times older than 20 Ma. In theory this model provides improved constraints on absolute plate motion because it does not solely rely on hotspots or palaeomagnetic data. Instead van der Meer et al. (2010) correlate geological data related to the initiation or cessation of subduction at the surface to deep mantle structures, using a total of 28 slabs imaged by p-wave tomography. They attempt to relate the surface palaeo-position at key ages and the current depth of subducted slabs to each other, assuming that slabs sink vertically. They suggest that three well-imaged deep mantle anomalies are up to 18° longitudinally skewed to the east at 160 Ma relative to previously published reconstructions. They correct this apparent misfit by adding a time-dependent longitudinal shift to the hybrid TPW-corrected model.

## 3. Integrated geodynamic models

The hierarchical nature of the global platecircuits means that the absolute reference frame can be changed via a specific set of rotations for the African Plate. We place these absolute rotations into a reference global rotation file (Müller et al., 2008) containing relative rotations for all plates. All of these other plates are eventually linked to the global reference system through Africa and therefore changing the absolute motion of Africa will also change the location of all other plates. The relative rotations by comparison, remain identical for all plate models.

The only exception to this plate circuit is the Panthalassa Ocean region (pre-Pacific configuration, comprising the Farallon, Phoenix and Izanagi plates), which is more difficult to constrain because the plates of Panthalassa were completely surrounded by subduction zones prior to ~83.5 Ma. Therefore, before 83.5 Ma Panthalassa plates cannot be directly related to the rotation of Africa (via Marie-Byrd Land-Antarctica) and must be linked directly to an absolute reference frame. For the five 140 Ma models we use stage rotations for the plates within Panthalassa for times before 83.5 Ma from a plate model WHK06 (Wessel et al., 2006). This also means that if the hotspots and subsequent rotations used in WHK06 were not fixed, then the resulting motions of Panthalassa plates, and dependent plates, may not be identical to the motion of those plates relative to the spin axis. Furthermore, a major limitation is the lack of published constraints for the motion of plates within Panthalassa, especially for times before 100 Ma when reconstructions for the Pacific are poorly constrained. This uncertainty is relevant for imposed surface kinematics, including subduction, around the Pacific and therefore imposes limitations on our geodynamic models.

We utilize a set of topological plate boundaries (Gurnis et al., 2012) which are coupled to a specific set of rotations for each absolute plate motion model. These plate boundaries are imposed as closed plate polygons in 1 Myr intervals using the global plate tectonic reconstruction software GPlates (http://www.gplates.org; Boyden et al., 2011). The polygons are delineated by plate boundaries, comprising subduction zones, mid-ocean ridges and transform boundaries. The model-specific global plate boundaries and associated plate velocities at initial conditions are then imposed as time-dependent surface boundary constraints.

We also include three additional geodynamic models (Table S2) that have variable imposed surface plate motion from 200 Ma, also initialized since 300 Ma. The first is a fixed hotspot model (Müller et al., 1993) that keeps Africa fixed between 200 and 132 Ma as there are no hotspot tracks with clear age progression in the Atlantic/Indian oceans for times before 132 Ma and minimal absolute motion of Africa during this time period is also supported by other models (Steinberger and Torsvik, 2008; Torsvik et al., 2008). The second is the hybrid TPW-corrected model (O'Neill et al., 2005; Steinberger and Torsvik, 2008) and the third is the subduction reference frame (van der Meer et al., 2010). The inclusion of these forward geodynamic models allows us to investigate the cause of lowermost mantle heterogeneity, as we find that using our mantle parameters, a slab subducted at 140 Ma is unlikely to have reached depths greater than ~2600 km (see also, Section 4.2). These 200 Ma models differ from the 140 Ma set as they incorporate an updated plate kinematic model (Seton et al., in review) and use the WK08-G Wessel and Kroenke (2008) absolute plate motion model for the Pacific for times before 83.5 Ma. Some notable differences between models WK08 and WHK06 are that WHK06 does not include the mid-Pacific mountains as constraints, whereas WK08 does and the extinct hotspot locations for the northern and southern Shatsky rises differ slightly between models. While not the focus of this study, we demonstrate a fundamental difference between the modelled circum-Pacific mantle structure based on alternative absolute Pacific plate motions inherent in these two published models.

We compute our mantle circulation models (MCMs) using the parallel finite element TERRA code (Bunge et al., 1996, 1997; Oeser et al., 2006). TERRA solves for the momentum and energy balance at infinite Prandtl number (i.e. no inertial force) in a spherical shell with global grid spacing of ~25 km. Compressibility effects are incorporated in form of the anelastic liquid approximation. The high numerical resolution allows us to model mantle flow at Earth-like convective vigour, expressed by a thermal Rayleigh number of ~$10^9$ based on internal heating (e.g. Bunge et al., 1997). MCM input parameters (Table 1) are equivalent to Schuberth et al. (2009a).

Our MCMs assume a three-layer viscosity profile, identified as the lithosphere, upper mantle and lower mantle, separated at 100 and 650 km depth. The assigned viscosities are $10^{23}$, $10^{21}$ and $10^{23}$ Pas, respectively. The effects of phase transitions on mantle flow dynamics are not included in our simulations. Our choice of mechanical boundary conditions is free-slip at the CMB (the core supports no shear-stress), while velocities at the surface are specified in accordance with the plate motion models. Temperature is kept constant at the surface (300 K) and CMB (4200 K), with the CMB temperature chosen to yield global mantle flow with strong plume flux (Bunge, 2005). A dynamic regime dominated by thermal structure provides a good match to seismic tomography in terms of heterogeneity strength (Schuberth et al., 2009a) and radial profiles (Styles et al., 2011). The unknown initial conditions of mantle heterogeneity are approximated by running convection from 300 Ma with global plate configurations fixed to the oldest available reconstruction of each absolute plate motion model so as to generate a quasi steady thermal state (Bunge et al., 2002).

**Table 1**
Mantle parameters for Terra models.

| Parameter | Value |
|---|---|
| Outer radius | 6370 km |
| Inner radius | 3480 km |
| Temp at surface | 300 K |
| Temp at CMB | 4200 K |
| Reference viscosity | $10^{21}$ Pa s |
| Thermal conductivity | 3.0 W $m^{-1}$ $K^{-1}$ |
| Thermal expansivity at surface | $4.011 \times 10^{-5}$ $K^{-1}$ |
| Thermal expansivity at CMB | $1.256 \times 10^{-5}$ $K^{-1}$ |
| Internal heating rate | $6.0 \times 10^{-12}$ W $kg^{-1}$ |
| Heat capacity | $1.134 \times 10^{3}$ J $kg^{-1}$ $K^{-1}$ |
| Rayleigh number | ~$10^9$ |

The modelled geodynamic mantle heterogeneity for each of the absolute plate models can be compared to seismic tomography. To this end we map MCM thermal structure into corresponding elastic shear velocity anomalies, taking advantage of a published thermodynamically self-consistent model of mantle mineralogy in the CFMAS (CaO–FeO–MgO–$Al_2O_3$–$SiO_2$) system (Stixrude and Lithgow-Bertelloni, 2005, 2007). A pyrolite bulk composition is considered, consistent with our assumption of whole mantle flow, when we convert the pressure-temperature condition at each model grid point to its corresponding shear velocity.

An important element in the analysis of MCM heterogeneity is the resolving power of seismic tomography (Mégnin et al., 1997), which affects the spectral characteristics of mantle structure especially in regions of poor ray coverage (Bunge and Davies, 2001). We follow Schuberth et al. (2009b) and consider the effects of uneven data coverage and damping inherent in model S20RTS (Ritsema et al., 1999, 2004) by "tomographically filtering" our MCMs to S20RTS, that is we multiply the geodynamic mantle structure with the resolution operator R of S20RTS (Ritsema et al., 2007). As we are focused on comparing long-wavelength features, we find the published workflow using S20RTS to be appropriate for our study. The tomographically filtered MCMs match S20RTS in terms of the magnitude of seismic shear velocity variations (Schuberth et al., 2009b).

To further quantitatively describe differences in predictions of mantle structure for each absolute reference frame at a given depth, we correlate locations of subducted material predicted by our tomographically filtered MCMs. The slab structures, represented as closed polygons in map view at a given depth, are derived from contours from a particular seismic velocity perturbation e.g. 0.5%, for each of the datasets i.e. S20RTS versus each of the seismically filtered geodynamic models. The quality of fit is based on intersecting the seismic velocity polygons and the filtered geodynamic model polygons in spherical coordinates and considers two performance measures, assessing both the accuracy of the fit, and the fit residual respectively (Further methodology in SOM). This is then used to generate rankings for each of the models as compared to S20RTS. We apply this technique both globally and regionally, at a range of depths and contour values. We note that the regional comparisons in particular may be affected by the fact that we neglect certain aspects important for mantle dynamics; a more realistic rheology or including the dynamic effects of phase transition may change the exact location and shape of structures (on the order of tens to a few 100 kms at most). However, we modify our predictions to reflect the long-wavelength nature of tomography on the order of ~1000 km, so that more realistic flow models will likely not give very different results.

## 4. Results and discussion

### 4.1. Plate polygons and velocities

A crucial element to forcing slab subduction of MCMs is through the imposition of surface plate velocities and subduction boundaries. At 200/140 Ma, the surface plate velocities and subduction zone locations serve as initial conditions for our geodynamic models and are therefore first-order drivers in the lowermost mantle heterogeneity. Between 200/140 and 100 Ma, alternative absolute plate motion models display significant differences in imposed rotations and therefore the greatest variation in imposed surface kinematics. In contrast, between 100 and 0 Ma the plate rotations for alternative absolute reference frames are identical, with the exception of the fixed hotspot and subduction reference models.

Changes in absolute reference frame hold three main implications for surface constraints in our MCMs, (1) plate velocity magnitude, (2) plate velocity direction and (3) plate boundary location, especially subduction zones (Figs. 1–3). These variables determine the amount, rate and location of slab subduction in the mantle as predicted by our MCMs. Global velocity vectors computed for each plate at initial conditions (Figs. 1, 2), illustrate significant differences in velocity magnitude and direction between the models.

Surface kinematics at 140 Ma (Figs. 1, 3) contrast the hotspot models (fixed and hybrid hotspot models) and the hybrid models (hybrid palaeomagnetic, hybrid TPW-corrected and subduction reference models). This is unsurprising considering that at this time the hotspot models are based on similar datasets, namely the African hotspots, whereas the remaining models are based on palaeomagnetic data. For instance, in the eastern Pacific, the hotspot models show an oblique but largely convergent margin between the overriding North and South America plates and the subducting Farallon and Phoenix plates. By contrast, the hybrid models display relatively more oblique convergence along the eastern Pacific margin. For instance, the NAM and Farallon plates at 140 Ma are travelling in a similar northerly direction, while the South American (SAM) margin is weakly divergent in a north to north–east direction. In particular, the hybrid palaeomagnetic model shows NAM and SAM travelling at a faster velocity, over 10 cm/yr, than the adjacent oceanic plates, ~8 cm/yr. The same trend is predicted at 200 Ma (Fig. 2) comparing the fixed hotspot model with the hybrid TPW and subduction models. Such oblique convergence dynamics at these subduction boundaries would lead to reduced volumes and rates of slab subduction, compared to the hotspot models.

Another major area of discrepancy between the velocities of the models at 200 and 140 Ma is Eurasia. At 140 Ma, the hotspot and the subduction reference models predict similar velocities to each other (~1 cm/yr), in an overall southerly direction, whereas the hybrid palaeomagnetic and TPW-corrected models predict an east–southeast motion. In particular, the hybrid palaeomagnetic model shows fast velocities (in excess of 9 cm/yr). These observations also hold implications for the amount and age-depth correlation of subducted slabs under Eurasia. Similarly, at 200 Ma, the hybrid TPW-corrected and subduction models predict faster velocities for the Eurasian plate than the fixed hotspot model.

A comparison of the relative positions of global plate boundaries illustrates the effect of different absolute plate rotations (Fig. 3). As expected, the 140 Ma hybrid palaeomagnetic and TPW-corrected models are relatively similar in plate boundary location, with an offset of no more than 5–10° in either longitude or latitude. The hotspot models are also similar to each other with up to 5–10° offset in longitude or latitude. Comparing the hotspots against hybrids, there are offsets in the equatorial and mid-latitudes of up to 15° in latitude and 10° longitude. In the higher latitudes, the longitudinal offset between these models is greater, with up to 60° variation in longitude (>3000 km). These discrepancies are particularly important for subduction zone boundaries through time, as they determine the location of slab emplacement and the resultant temperature distribution throughout the mantle.

While there are significant offsets in longitude between all models, the plate boundaries of the subduction reference frame are particularly different, with up to 5–30° offset from the other absolute reference frames. Even though the rotations are based on the hybrid TPW-corrected model, the correction of longitude according to lower mantle slab location has led to large shifts in plate boundary longitude.

Some of the largest discrepancies in plate-boundary locations at both 200 and 140 Ma are around the Pacific margin. For instance, along the NAM and southwest Pacific subduction margins there is an offset of ~30° longitude between the models, and the northwest Pacific margin shows an offset of up to ~60° longitude (>3000 km). There is also a significant north–south offset between the models along the southern Eurasian margin of up of ~20°. In particular, this margin appears to contrast the hotspot models against the hybrid models.

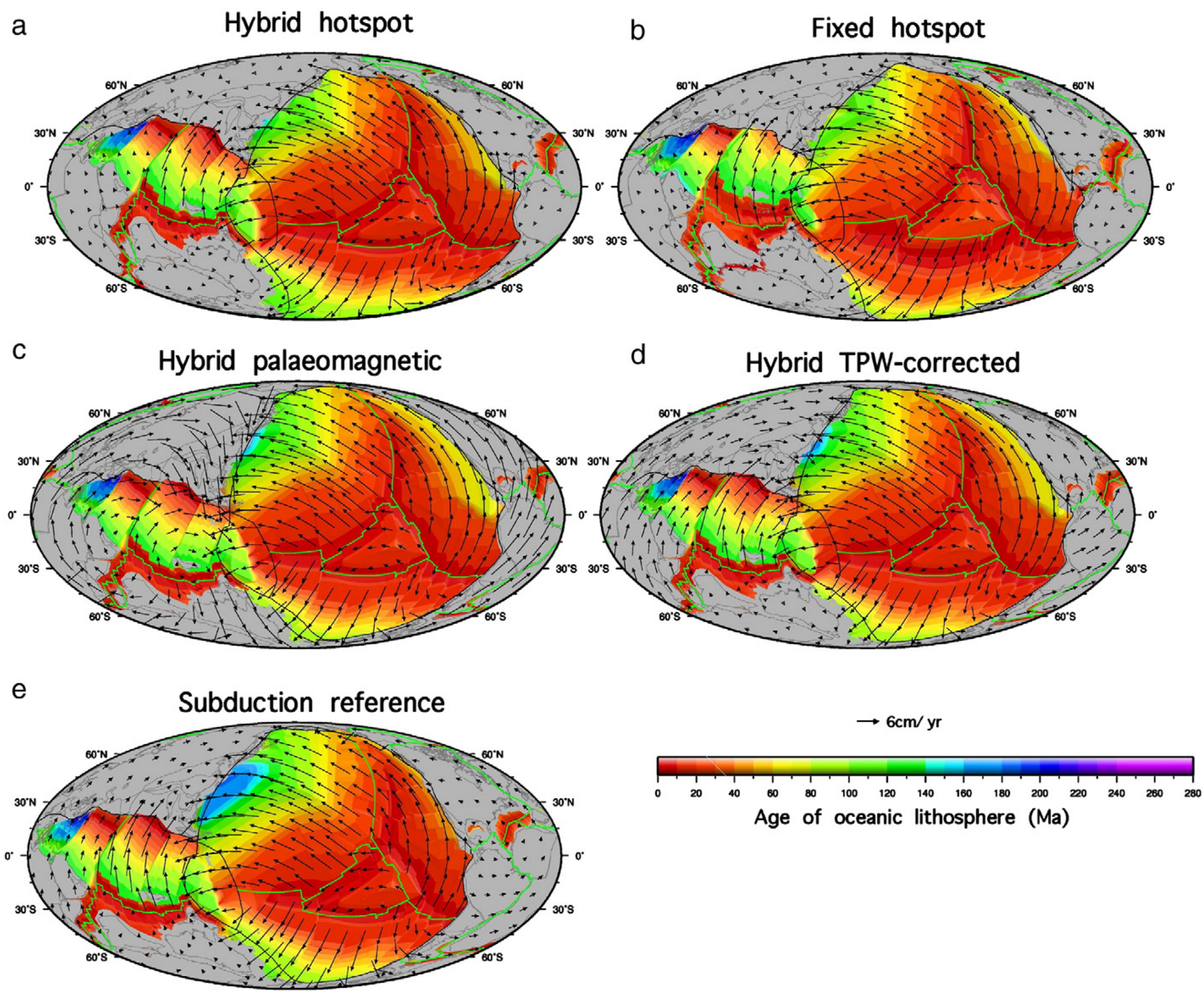


**Fig. 1.** Comparison of global plate boundaries and plate velocities with associated age grids for the five absolute reference frame models at 140 Ma initial conditions. The age-grids were calculated using time-dependent synthetic isochrons rotated according to the absolute plate motion model.

*4.2. Mantle sinking rates*

Based on our geodynamic model setup with an upper/lower mantle viscosity contrast of 100 and the governing equations of mantle flow, we can relate the depth of slab material from our geodynamic models to a particular age of subduction. Furthermore, the use of a radial increase in viscosity leads to the subducted slabs sinking sub-vertically. We find that sinking velocities in the upper mantle are typically 5 cm/yr and those in the lower mantle do not exceed 1.5–2 cm/yr. Using these values we find that subducted material at ~2000 km depth corresponds to a subduction age of 100 Myrs, at ~2600 km to 140 Myrs and at the CMB to ~160 Myrs. The global correlation of filtered model output to tomography model S20RTS (Fig. 7, subpanel f) illustrates that the mantle-averaged correlation of the models diverges below ~1800–2000 km depth. We interpret this divergence to correspond to the depth where the absolute plate motions differ the most i.e. times older than 100 Ma.

The greatest variation in absolute reference frames occurs between 200/140 and 100 Ma, and we therefore expect that as depth increases so will variation in mantle structure. We find, however, that the initialization process has some impact on the structure of the entire mantle, even at relatively shallow depths associated with more recent times of subduction, when the surface kinematics across the models are similar. Additionally, it must be considered that due to initialization we only vary surface kinematics for the five 140 Ma models for times younger than 140 Ma. Therefore, to interpret the geodynamic structure of slabs with ages older than ~100–140 Ma (depths below 2093–2550 km), we primarily use the 200 Ma models. Notably, when we compare palaeo-plate boundaries at 200 Ma from the TPW-corrected model to those at 140 Ma (Fig. 3) we find that the location of subduction zones along NAM and SAM is largely stable, whereas locations such as southern Eurasia and the western Pacific are highly variable, with 15–30° difference in longitude and latitude.

*4.3. Mantle heterogeneity structure*

High temperature contrasts (on the order of several hundred degrees Kelvin) (Figures S3, S4) demonstrate that the thermal heterogeneity of our forward modelled lower mantle is a function of variable surface constraints (Figs. 1–3). To best compare our modelled mantle heterogeneity we have tomographically filtered the geodynamic model output for each absolute reference frame (Figs. 4, 5). The raw output, displaying thermal mantle structure, can be found in the SOM (Figures S3–S6).

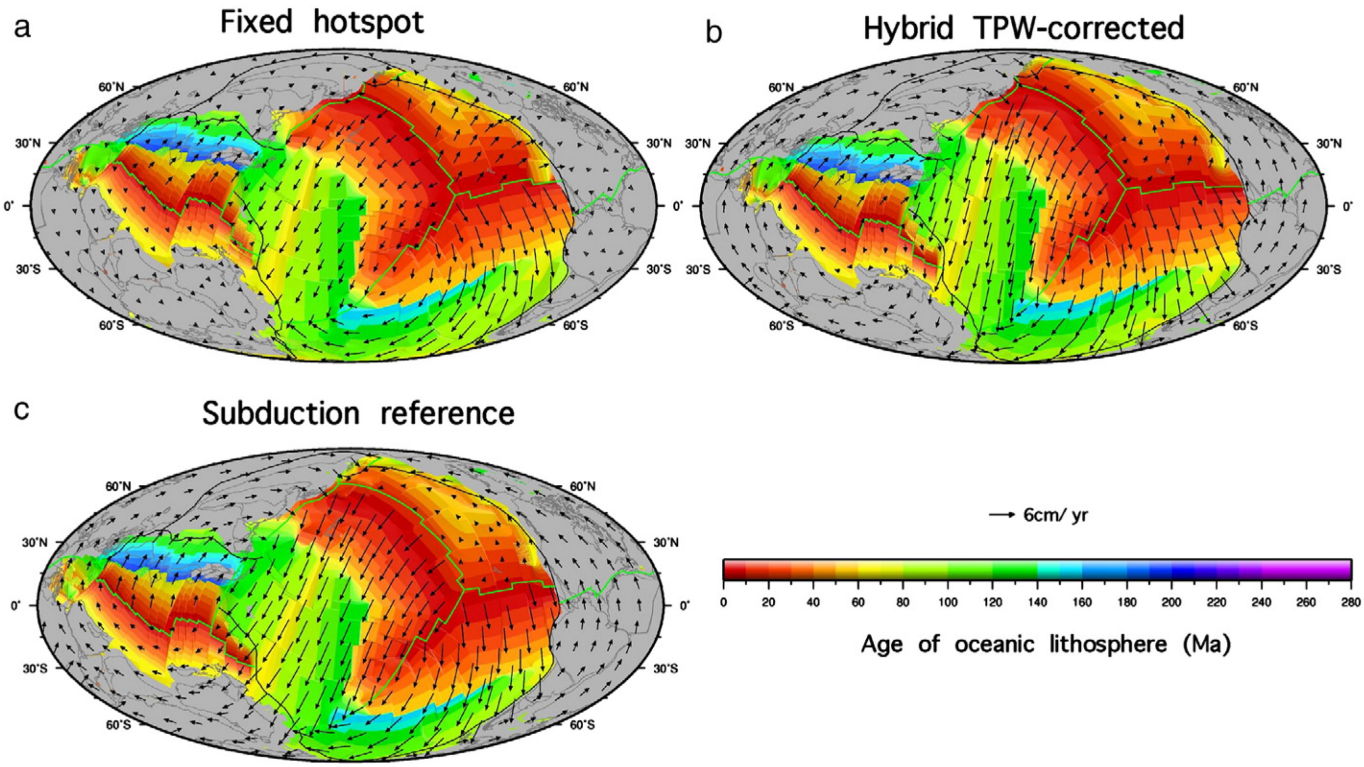


**Fig. 2.** Comparison of global plate boundaries and plate velocities with associated age grids for the three absolute reference frame models at 200 Ma initial conditions. Note that at 200 Ma the plates within Panthalassa are tied to the absolute reference frame via Africa from 200 to 190 Ma.

Forward predicted mantle structure from 1875 to 2550 km (Fig. 4) for the 140 Ma models differs significantly between the absolute reference frames in two main regions, namely, the eastern and western margins of the Pacific. Along the eastern Pacific margin, the hotspot models both predict significant amounts of subducted slab material under NAM and SAM. There is, however, a break in slab material at 30–40°S, which can be accounted for by the subduction of the Farallon–Phoenix mid-ocean ridge. In contrast, the hybrid models (hybrid palaeomagnetic, TPW-corrected and subduction reference) predict minimal slab material in this entire region under NAM and SAM (from ~20°N–40°S). This can be attributed to the relative velocities between the overriding NAM and SAM plates relative to the subducting Farallon and Phoenix plates (Figs. 1, 2). As noted in Fig. 1, the oblique convergence along this boundary would lead to reduced volumes and rates of subducted oceanic lithosphere. The overall mantle structure in this region as imaged by S20RTS appears to better match that predicted by the hotspot models.

Across the western Pacific, the modelled pattern is more variable. However, the hotspot models predict greater volumes of slab material, especially in the eastern regions of Eurasia, whereas the hybrid palaeomagnetic model predicts the least amount of slab material under eastern and central Eurasia. This is also evident in the temperature output (Figure S3). The predictions of mantle heterogeneity can loosely group the absolute reference frames into two distinct groups; the hotspot models, and the hybrid models.

It is interesting that under the eastern Pacific, where the locations of plate boundaries are shown to be the most stable between 200 and 140 Ma (Fig. 3), there are significant differences in slab heterogeneity as predicted with the five 140 Ma models. By contrast, regions where plate boundaries are the most variable through time, such as under the northwestern Pacific, show more subtle differences in mantle structure. In other words, while the location of slab material is variable within a given region, the presence of slab material at all is a significant difference between the models. This suggests that first order differences in forward predicted mantle structure are due mostly to palaeo-plate velocities rather than plate boundary location.

Unlike the 140 Ma models, the heterogeneity of the lower mantle (1875–2791 km) from all three 200 Ma models shows significant accumulations of slab material under NAM and SAM. This can be attributed to the use of the WK08 132–144 Ma absolute stage rotation for modelling Pacific absolute motion prior to 144 Ma, resulting in convergence dynamics along this margin between 200 and 140 Ma that are dramatically different from using the WHK06 model. The resulting slab heterogeneity matches the mantle structure in this region as observed by S20RTS substantially better, suggesting WK08 is a more appropriate reference model than WHK06 for modelling the absolute motion of the Pacific and adjacent plates for times before 100 Ma. This result highlights that our approach allows us to use forward geodynamic modelling of lower mantle structure to test absolute reference frames for the Pacific that are ill-constrained from hotspot track data alone.

The two main anomalously hot regions throughout the mantle under central Pacific and Africa across all models can be interpreted as related to the Large Low Shear Velocity Provinces. Their generation in all of our geodynamic models, which are initialized with a random mantle temperature field and imposed surface kinematics, suggests that these features are mantle-convection and/or subduction generated rather than solely post bollide impact reservoirs of mantle heterogeneity (Burke et al., 2008; Tolstikhin and Hoffmann, 2005). While our models are dominated by changes in mantle temperature, it is possible that these structures represent compositional heterogeneity e.g. thermo-chemical piles. Furthermore, the 200 Ma models predict slab material further towards the centre of Panthalassa compared to the 140 Ma models, despite no imposed subduction boundaries existing that far west during the last 200 Myrs. This is an interesting observation, suggesting that flow dynamics may contribute to anomalously displaced slab material, and that a plate boundary at the surface is not necessarily required to produce such deep mantle structure offset from known convergent boundaries (van der Meer et al., 2010).

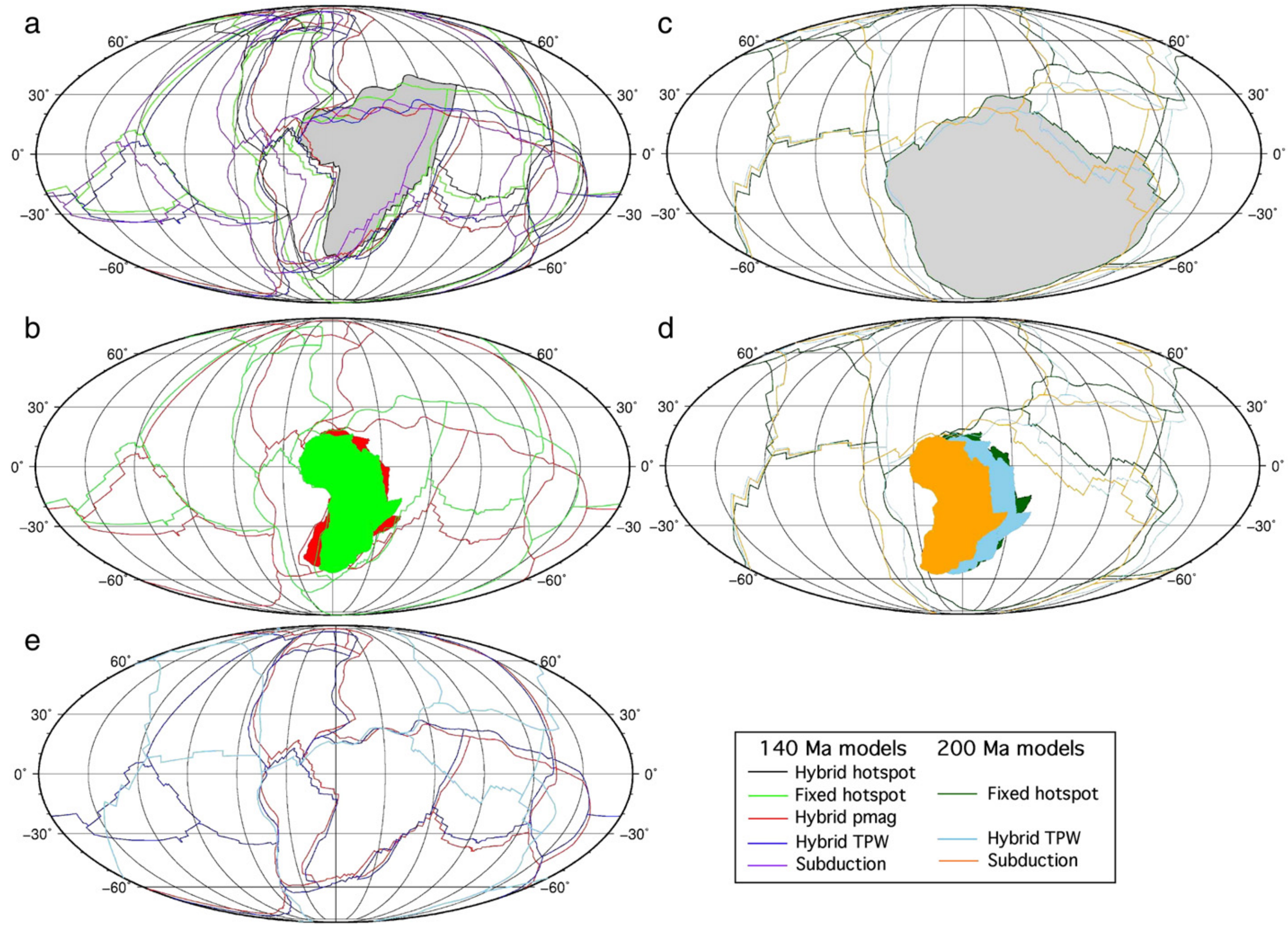


**Fig. 3.** The 140 Ma models: (a) Locations of reconstructed palaeo-plate boundaries for the five absolute plate motion models at initial 140 Ma conditions centred on the African Plate, which is shaded grey for the hybrid hotspot model. (b) Comparison of palaeo-plate boundaries from just the fixed hotspot and hybrid palaeomagnetic models, with African continent shaded for comparison. The 200 Ma models: (c) Locations of reconstructed palaeo-plate boundaries for the three absolute plate motion models at 200 Ma initial conditions centred on the Gondwana Plate, which is shaded grey for the fixed hotspot model. (d) as with (c) but with African continent shaded for comparison. Both sets: (e) Comparison of palaeo-plate boundaries at 140 Ma from the hybrid palaeomagnetic and hybrid TPW-corrected models, and the TPW-corrected model at 200 Ma. See inset for legend.

### 4.4. Regional comparison

While we have established that the longitudinal and latitudinal positioning of global palaeo-plate boundaries are highly variable according to absolute reference frame (Fig. 3), the discrepancies across major subduction zones provide the most interesting regional comparison between absolute reference frames. The western NAM and southern Eurasian margins are long-lived subduction zones and show significant longitudinal and latitudinal differences in both the location of plate-boundaries and forward-predicted mantle structure according to absolute reference frame used.

The eastward-dipping Farallon slab is consistently imaged across various P and S-wave tomography models as well as our MCMs (Fig. 6). The correlation of the Farallon slab as imaged by seismic tomography is arguably best reproduced to the first-order by the (200 Ma) fixed hotspot model, and to a lesser extent, the hybrid TPW-corrected model. The Farallon slab in these models appears to better capture the geometry and overall location of the equivalent tomography slab, despite being offset in depth and/or longitude. The offset in depth may be accounted for by the viscosity profile imposed, and therefore associated slab sinking rates, whereas the longitudinal offset may be accounted for by the absolute reference frame. The 140 Ma hotspot models also show a good correlation of the Farallon slab (Figure S7). Our results suggest that the constraints on palaeo-longitude applied from hotspot models are reasonable.

By contrast, the Farallon slab as modelled in the subduction reference model and the 140 Ma hybrid models (Figure S7) are offset to the west compared to tomography. With the exception of the subduction model, this longitudinal offset in the mantle is at odds to the location of the palaeo-plate boundary locations at 140 Ma (Fig. 3), whereby the hybrid models are located further east than the hotspot models. This again suggests that palaeo-plate boundary location is not the main driver in lower mantle slab heterogeneity but rather surface plate velocities and subduction zone evolution. The offset of the subduction reference model to tomography suggests that the longitudinal corrections it applies are perhaps too great for times after 140 Ma.

The surface location of the southern Eurasian plate boundary at initial conditions (Fig. 3), shows a latitudinal contrast between the hotspot models and the hybrid palaeomagnetic and TPW-corrected models of up to 15°. The subduction reference frame boundary retains a comparable latitude to the hybrid models, but is offset further west. While this latitudinal offset is not particularly evident in the vertical cross-sections through this margin for the 200 Ma models (Fig. 6), it is modelled in the 140 Ma models (Figure S7). This latitudinal slice also images the stalling of slabs in the hotspot models at approximately 1800 km depth. By contrast the hybrid models image significantly more material in the lowermost mantle, and are located

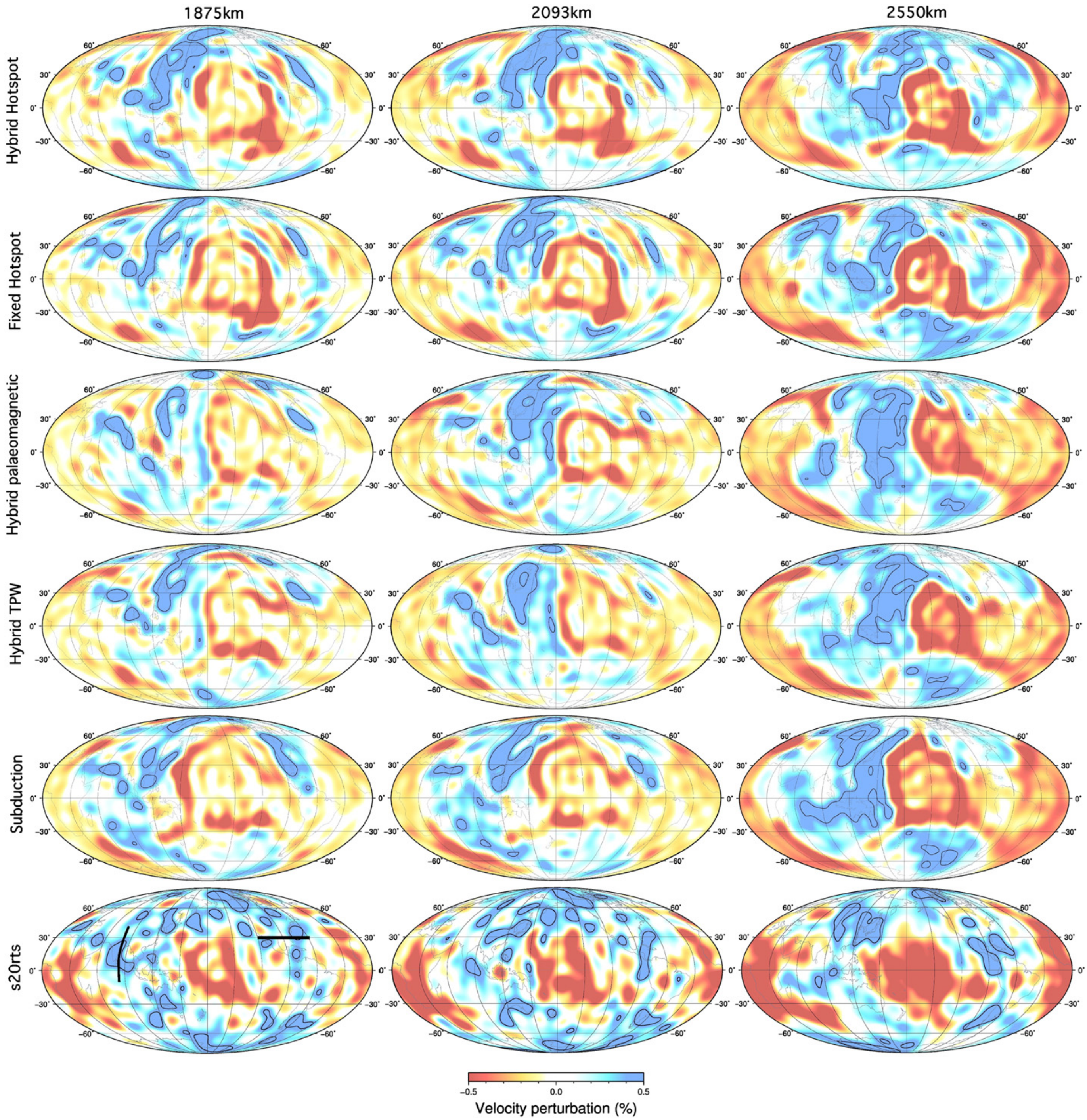


**Fig. 4.** Tomographically filtered forward model output from 1875 km (~90 Ma), 2093 km (~100 Ma), and 2550 km (~140 Ma) for the five 140 Ma absolute reference frame models and S20RTS tomography model, with present-day coastlines imposed for reference. 0.5% seismic velocity perturbation is contoured in black for each subplot. Positive seismic anomalies (blue) are inferred to represent subducted slab remnants. Thick black lines in bottom subfigure denote the location of the vertical slices in Fig. 6. Note, the relative absence of subducted material beneath South America in the hybrid models (hybrid palaeomagnetic, TPW-corrected and subduction reference frame). (For interpretation of the references to colour in this figure legend, the reader is referred to the web version of this article.)

further towards the south. This arguably matches tomography better than the hotspot models, especially in the lower mantle. This discrepancy suggests that the hotspot models are not as well constrained in latitude, especially for times older than ~80 Ma.

### 4.5. Correlation to seismic tomography

To further investigate the differences between the MCMs and seismic tomography we apply two correlation techniques. The first uses spherical harmonics, and shows that most significant differences in modelled mantle thermal structure between the absolute reference frames occur on the largest hemispherical scales i.e. spherical harmonic degrees 1–3, which correspond to a wavelength of resolved features from ~6600 to 20,000 km in width. At these harmonic degrees for the 140 Ma models, the fixed hotspot model (Fig. 7) shows the highest degree of correlation to S20RTS, particularly in the upper mantle between 300 and 1500 km depth (0 to ~60 Myrs of subduction). The subduction reference frame shows an intermediate

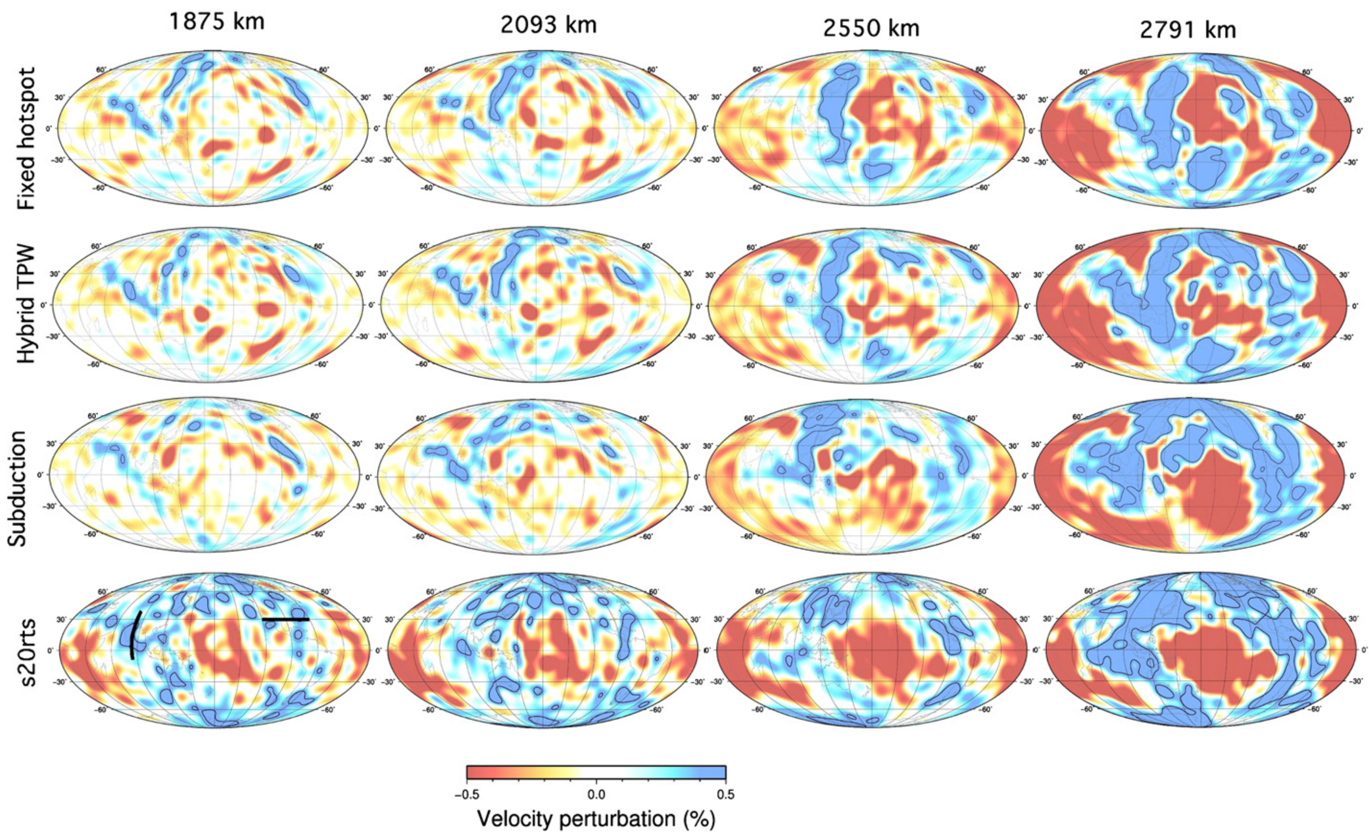


**Fig. 5.** Tomographically filtered forward model output from 1875 km (~90 Ma), 2093 km (~100 Ma), 2550 km (~140 Ma) and 2791 km (~200 Ma) for the three 200 Ma absolute reference frame models and S20RTS tomography model, with present-day coastlines imposed for reference. 0.5% seismic velocity perturbation is contoured in black for each subplot.

degree of correlation for the upper mantle, but decreases sharply between 2000 and 2791 km depth. By contrast, the 200 Ma fixed hotspot and TPW-corrected models (Fig. 8) show a similar depth-correlation trend to each other. Notably, the subduction reference frame improves significantly in the lower mantle (below ~2000 km depth) predicting a superior performance compared to the other two models. These observations, however, are only globally averaged and do not provide information as to the azimuth of these discrepancies i.e. longitude or latitude, or about their regional distribution.

As an alternative analysis we investigate the area of intersecting polygons derived from seismic tomography and each of the seismically filtered models (Figure S8). Using this technique, we find that at a given depth, the fit score rankings are highly dependent on the threshold/contour values used e.g. 0.5% seismic perturbation (Figures S8, S9, Tables 2, 3, S3–S18). Figure S8 shows that the wavelengths of subducted slabs captured across these thresholds (e.g. range of ~200–4000 km at 0.5% perturbation) are much smaller than the 1–3 spherical harmonics wavelengths. As expected, as the threshold

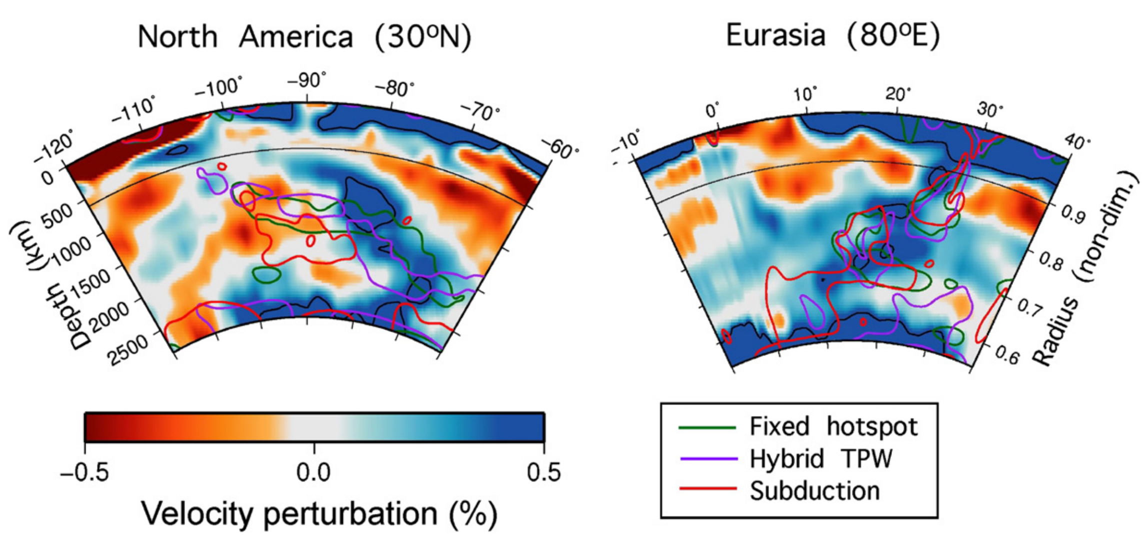


**Fig. 6.** Vertical slice through North America (30°N) and southern Eurasia (80°E) (see Fig. 4 for locations) from Grand's (2002) tomography model contoured at 0.5% seismic velocity deviation (black line), superimposed with the −300 K temperature perturbation contour as predicted by the three forward geodynamic models from 200 Ma (Figure S6), see inset for legend.

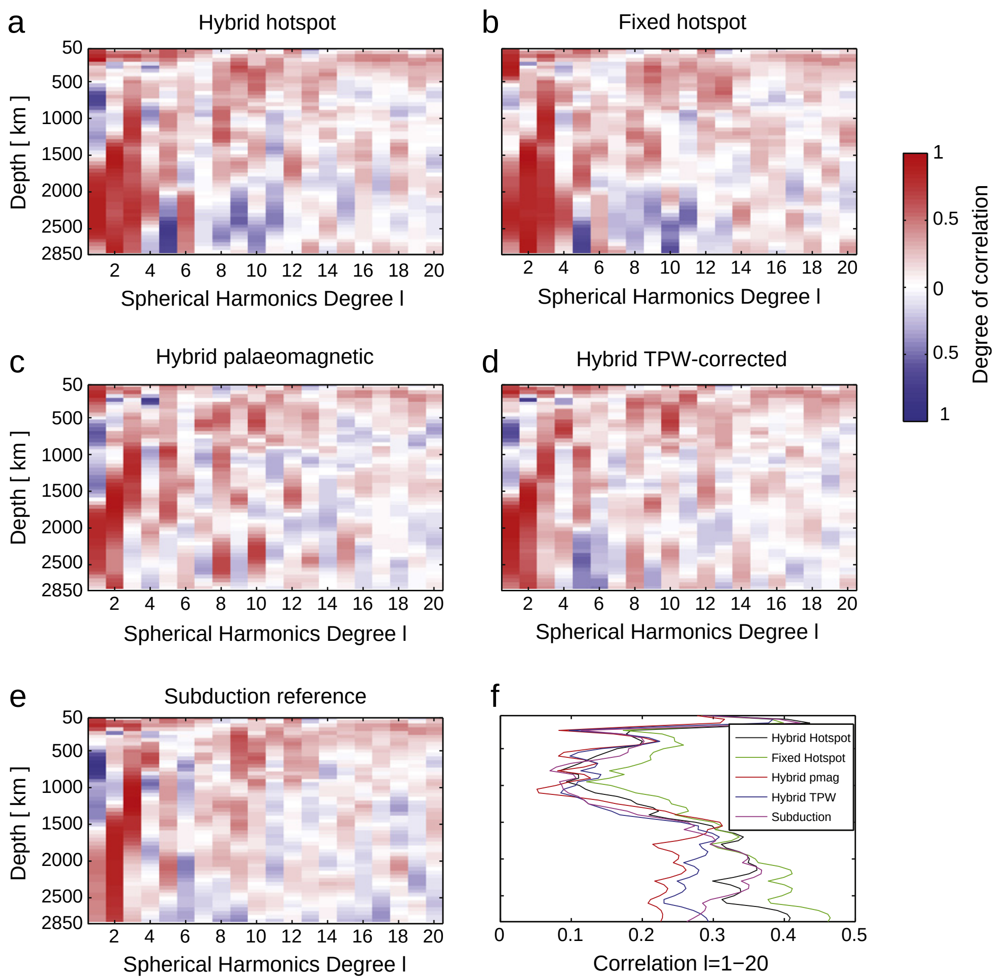


**Fig. 7.** Spectral heterogeneity comparison of geodynamic mantle structure (tomographically filtered seismic velocity perturbations) for the five 140 Ma models to tomographic model S20RTS for spherical harmonic degrees 1–20 (a) hybrid hotspot, (b) fixed hotspot, (c) hybrid palaeomagnetic, (d) hybrid TPW-corrected, (e) subduction reference frame and (f) average correlation of degrees 1–20 for all models. The colour scale indicates the degree of correlation (between −1 and 1) between the relative velocity variations, and plotted as a function of spherical harmonic degree and depth. Lowermost depths (below ~2550 km) may not be appropriately modelled due to initialization conditions.

increases, polygon area in both the geodynamic and tomography models decreases, and therefore the probability of intersection decreases, resulting in a lower fit score.

Using the global analysis (Fig. 9, Table 2) for the 140 Ma models, we find that at shallower depths i.e. 1445–2093 km, corresponding to times younger than 100 Ma, the hotspot, hybrid palaeomagnetic and TPW-corrected models cannot be easily distinguished. This may be expected considering these models impose the same, or similar, rotations for times after 100 Ma. Additionally, the correlation of the two hotspot models is very similar at global scales, suggesting that the motion of hotspots implicit in the O'Neill et al. (2005) model over the last 100 Myrs is not sufficiently different from a fixed hotspot model to result in significant differences in modelled mantle structure up to degree and order 20, which is what we consider here. However, it can be argued that the hybrid palaeomagnetic model generally outperforms the other models in fit score averaged value (Table 2) whereby it shows the highest correlation across all three averaged depth ranges. The global analysis for the 200 Ma models (Fig. 10, Table 3) suggests that the hybrid TPW-corrected/moving hotspot model, and the fixed hotspot model to a lesser extent, are more appropriate for shallower depths (less than 90 Ma), whereas the subduction reference is most appropriate for times older than 140 Ma.

In addition to the global analysis, we focus our polygon intersection analysis on the mantle beneath the long-lived subduction zones of NAM and southern Eurasia (Figures S11–14, Tables S7–S18). For the 140 Ma models, the subduction reference frame performs poorly compared to the remaining models, which cannot be easily distinguished. These depths, associated with subduction after 140 Ma suggest that the longitudinal correction applied by van der Meer et al. (2010) is too large, at least for these times. We note that while performing poorly for more recent times, the subduction reference model yields good results for lower mantle depths under Eurasia for both the 140 and 200 Ma models (Figures S12,S14). This suggests that constructing subduction reference frames by combining palaeomagnetic data with the geometry of subducted slabs provides a promising avenue for modelling the absolute motions of plates and plate boundaries for times where hotspot tracks are sparse or absent.

## 5. Conclusions

Our comparison of five alternative absolute plate motion models in terms of their consequences for deep mantle structure shows that there are notable differences in predicted mantle heterogeneity between different absolute plate motion models across a range of wavelengths. At long wavelengths (spherical harmonic degrees 1–3; or features up to 20,000 km in width) the hotspot models best reproduce the mantle structure. We suggest that the cause for the differences between plate models at the largest wavelengths is mostly due to differences in plate velocity. Furthermore, we find that

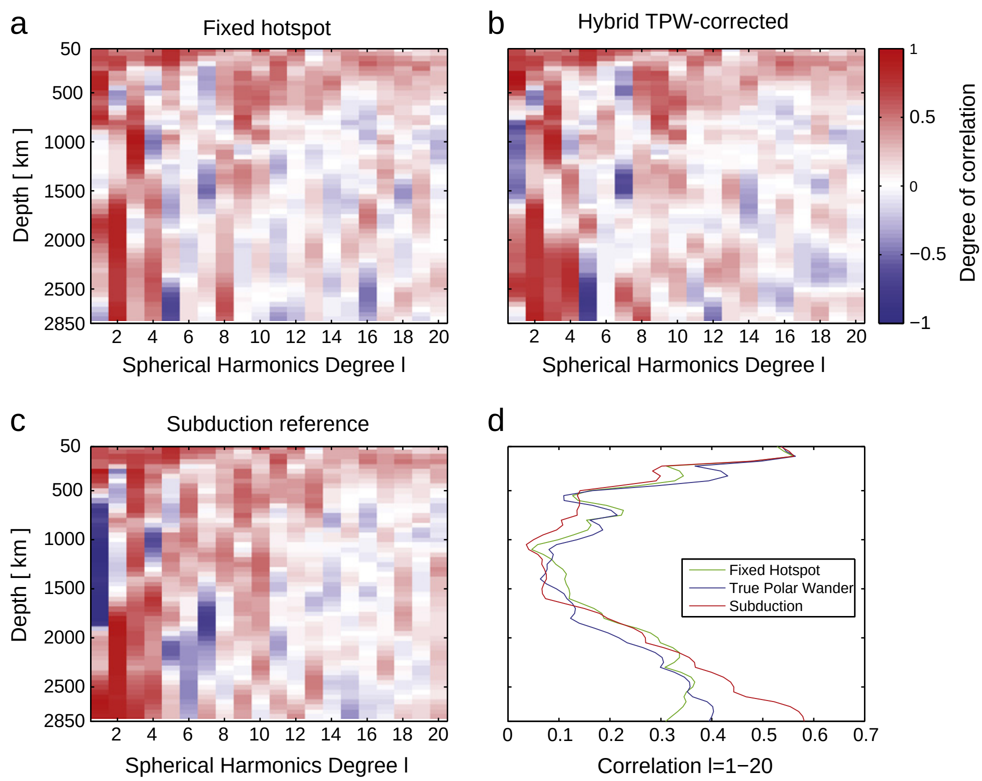


**Fig. 8.** Spectral heterogeneity comparison of geodynamic mantle structure (tomographically filtered seismic velocity perturbations) for the three 200 Ma models to tomographic model S20RTS for spherical harmonic degrees 1–20 (a) fixed hotspot, (b) hybrid TPW-corrected, (c) subduction reference frame and (d) average correlation of degrees 1–20 for all models. The colour scale indicates the degree of correlation (between −1 and 1) between the relative velocity variations, and plotted as a function of spherical harmonic degree and depth.

initialization conditions i.e. 200 vs 140 Ma hold first-order implications for mantle structure. We demonstrate that the use of a particular absolute reference frame for the Pacific holds significant implications for mantle heterogeneity. We find that the mantle structure modelled with a WK08 Pacific absolute reference frame is better correlated to S20RTS than WK06 in terms of eastern Panthalassa subduction dynamics.

When geometry and correlation of smaller-scale slab volumes are compared (less than 4000 km in width), the hybrid palaeomagnetic model (from the 140 Ma set) best reproduces the overall mantle structure of slab burial grounds, even though no single model fits best at all mantle depths. Differences in predicted plate boundary location may drive smaller wavelength offsets in modelled mantle structure as compared to other the absolute reference frames as well as to seismic tomography. We find the hybrid palaeomagnetic model to be the most robust absolute plate motion model compared to S20RTS at the wavelengths of subducted slabs and across most depths.

While the azimuthal coherence of the geodynamic models to S20RTS is poorly resolved and only discernible in the regional studies, we find that the hotspot models better reconstruct longitude than latitude, but only for times more recent than ~80 Ma. Such trends are less obvious in the hybrid models. However, the hybrid palaeomagnetic model is arguably better matched to S20RTS under Eurasia than under NAM suggesting it is better in latitude than longitude. This reflects the relative certainty from which palaeo-latitude is derived from palaeomagnetic data. Geodynamic modelling presents an independent means of testing palaeo-longitudes and latitudes, especially in the context of hotspot motion. Future studies of absolute plate motion should endeavor to incorporate such observations.

The consistent offset of the subduction reference frame to both seismic tomography and the other absolute reference frames, especially in longitude (e.g. under NAM) and for the upper mantle, suggests that the longitudinal corrections applied to this model are too great, for at least the last 140 Myrs. However, its improved performance in the lowermost mantle and in the 200 Ma models is strong evidence for its usefulness in plate models for times older than 140 Ma. We suggest that a combination of palaeomagnetics and

**Table 2**
Analysis of fit scores for the 0.5% contour for each of the five 140 Ma geodynamic models to S20RTS, globally averaged across three different depth ranges roughly corresponding to the time periods that reflect important changes in absolute plate motion rotations. Ranked according to the fit score for the 70–140 Ma period (first column).

| | 70–140 Ma (1445–2550 km) | 70–90 Ma (1445–1875 km) | 100–140 Ma (2093–2550 km) |
|---|---|---|---|
| Hybrid palaeomag | 0.28 | 0.35 | 0.23 |
| Fixed hotspot | 0.26 | 0.30 | 0.22 |
| Hybrid hotspot | 0.25 | 0.29 | 0.22 |
| Subduction | 0.23 | 0.23 | 0.23 |
| Hybrid TPW | 0.22 | 0.30 | 0.16 |

**Table 3**
Analysis of fit scores for the 0.5% contour for the three 200 Ma geodynamic models to S20RTS, globally averaged across three different depth ranges roughly corresponding to the time periods that reflect important changes in absolute plate motion rotations. Ranked according to the fit score for the 70–200 Ma period (first column).

| | 70–200 Ma (1445–2791 km) | 70–90 Ma (1445–1875 km) | 100–200 Ma (2093–2791 km) |
|---|---|---|---|
| Fixed hotspot | 0.33 | 0.30 | 0.35 |
| Hybrid TPW | 0.32 | 0.35 | 0.30 |
| Subduction | 0.29 | 0.19 | 0.37 |

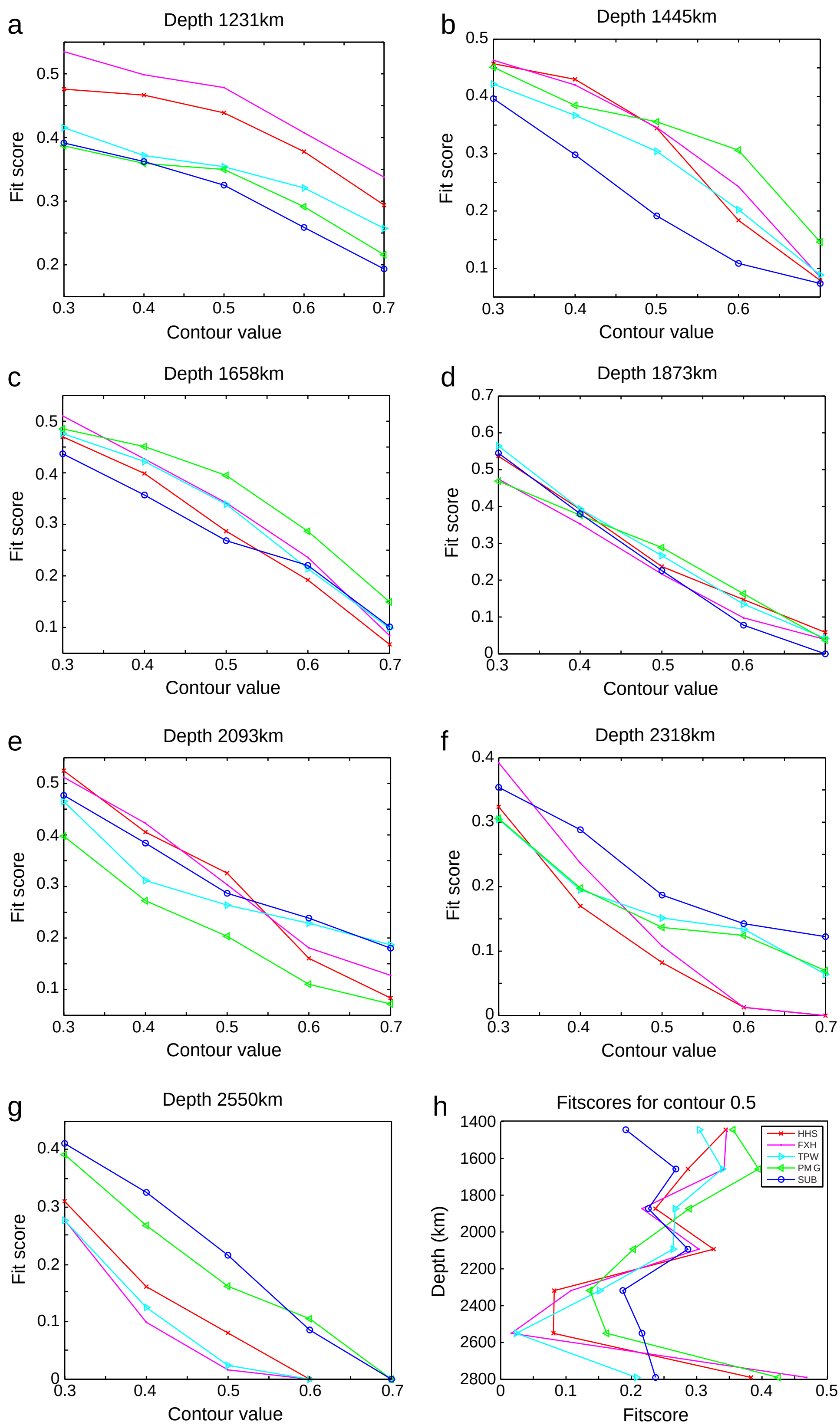


**Fig. 9.** Panels (a)–(g), Correlation fit scores from 1445 to 2550 km depth, and averaged for the entire globe, for each of the five 140 Ma seismically filtered geodynamic models to S20RTS for a given contour threshold value from 0.3% to 0.7% (the same for both data sets). The most reasonable window for direct analysis of intersecting polygons for subducted slab wavelengths is between 0.45 and 0.65% seismic velocity threshold, but outside values included to show trend changes on extreme scales. Fit scores from below 2550 km not included/analyzed due to poor resolution from the effect of initialization conditions.

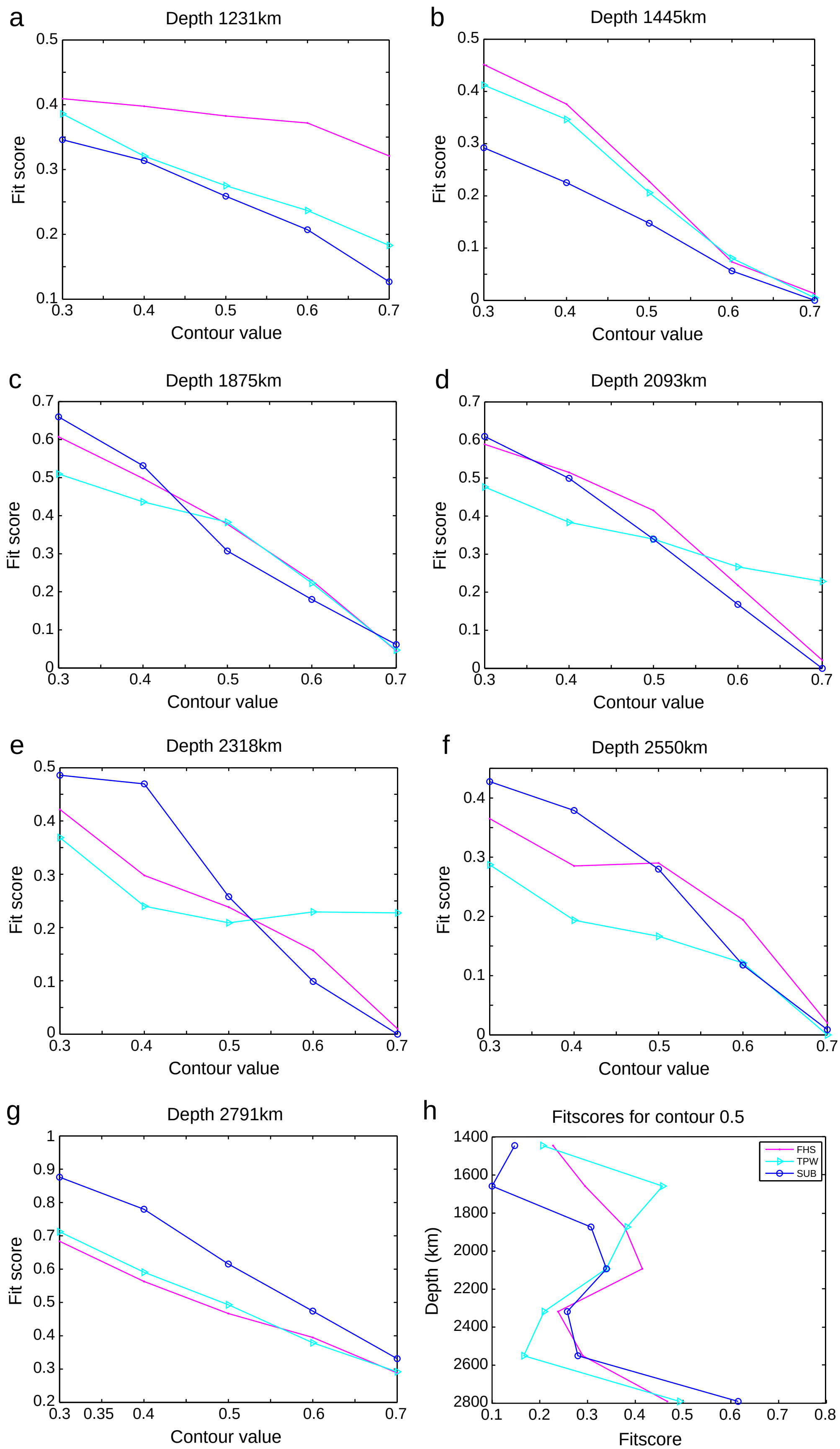


**Fig. 10.** Panels (a)–(g), Correlation fit scores from 1445 to 2791 km depth, and averaged for the entire globe, for each of the three 200 Ma seismically filtered geodynamic models to S20RTS for a given contour threshold value from 0.3% to 0.7% (the same for both data sets).

hotspots (for times after 100 Ma), together with geodynamic modelling, including inverse approaches for improved initial conditions (Bunge et al., 2003; Liu and Gurnis, 2008), to be used to construct an improved subduction reference frame.

## Acknowledgements

GES, RDM and AST were supported by Australian Research Council grants FL0992245 and LP0989312. BSAS was supported by a Marie Curie Intra European Fellowship within the 7th European Community Framework Programme [FP7/2007-2013] under grant agreement no. 235861. We thank the DEISA Consortium (www.deisa.eu), co-funded through the EU FP6 project RI-031513 and the FP7 project RI-222919, for support within the DEISA Extreme Computing Initiative. We would also like to thank Trond Torsvik for providing rotations for the subduction reference frame model.

## Appendix A. Supplementary data

Supplementary data to this article can be found online at doi:10.1016/j.epsl.2011.11.027.

A set of rotations and topologically closed plate polygons for the five alternative reference frames back to 140 Ma can be downloaded from ftp.earthbyte.org/papers/Shephard_etal_abs_ref_frames.

## References

Boyden, J.A., Müller, R.D., Gurnis, M., Torsvik, T.H., Clark, J.A., Turner, M., Ivey-Law, H., Watson, R.J., Cannon, J.S., 2011. Next-generation plate-tectonic reconstructions using GPlates. In: Keller, G.R., Baru, C. (Eds.), Geoinformatics: Cyberinfrastructure for the Solid Earth Sciences. Cambridge University Press, pp. 95–114.

Bunge, H.-P., 2005. Low plume excess temperature and high core heat flux inferred from non-adiabatic geotherms in internally heated mantle circulation models. PEPI 153, 3–10.

Bunge, H.-P., Davies, J.H., 2001. Tomographic images of a mantle circulation model. Geophys. Res. Lett. 28, 77–80.

Bunge, H.-P., Richards, M.A., Baumgardner, J.R., 1996. Effect of depth-dependent viscosity on the planform of mantle convection. Nature 379, 436–438. doi:10.1038/379436a0.

Bunge, H.-P., Richards, M.A., Baumgardner, R.A., 1997. A sensitivity study of three-dimensional spherical mantle convection at 10exp8 Rayleigh number: effects of depth-dependent viscosity, heating mode and an endothermic phase change. J. Geophys. Res. 102, 11991–12007.

Bunge, H.-P., Richards, M., Baumgardner, J., 2002. Mantle-circulation models with sequential data-assimilation: inferring present-day mantle structure from plate motion histories. Philos. Trans. R. Soc. London, Ser. A 360, 2545–2567. doi:10.1098/rsta.2002.1080.

Bunge, H.-P., Hagelberg, C.R., Travis, B.J., 2003. Mantle circulation models with variational data assimilation: inferring past mantle flow and structure from plate motion histories and seismic tomography. Geophys. J. Int. 152, 280–301.

Burke, K., Steinberger, B., Torsvik, T.H., Smethurst, M.A., 2008. Plume generation zones at the margins of large low shear velocity provinces on the core–mantle boundary. Earth Planet. Sci. Lett. 265, 49–60. doi:10.1016/j.epsl.2007.09.042.

Das, A.K., Piper, J.D.A., Bandyopadhyay, G., Basu Mallik, S., 1996. Polarity inversion in the Rajmahal lavas, north–east India: trap emplacement near commencement of the Cretaceous Normal Superchron. Geophys. J. Int 124, 427–432. doi:10.1111/j.1365-246X.1996.tb07030.x.

Davies, D.R., Davies, J.H., 2009. Thermally-driven mantle plumes reconcile multiple hot-spot observations. Earth Planet. Sci. Lett. 278, 50–54. doi:10.1016/j.epsl.2008.11.027.

Grand, S.P., 2002. Mantle shear-wave tomography and the fate of subducted slabs. Phil. Trans. R. Soc. Lond. A 360, 2475–2491.

Gurnis, M., Turner, M., Zahirovic, S., DiCaprio, L., Spasojevic, S., Müller, R.D., Boyden, J., Seton, M., Manea, V.C., Bower, D.J., 2012. Plate tectonic reconstructions with continuously closing plates. Computers and Geosciences 38 (1), 35–42. doi:10.1016/j.cageo.2011.04.014.

Idnurm, M., 1985. Late Mesozoic and Cenozoic paleomagnetism of Australia—II. implications for geomagnetism and true polar wander. Geophys. J. R. Astron. Soc. 83, 419–433. doi:10.1111/j.1365-246X.1985.tb06495.x.

Liu, L.J., Gurnis, M., 2008. Simultaneous inversion of mantle properties and initial conditions using an adjoint of mantle convection. J. Geophys. Res. 113, B08405. doi:10.1029/2008JB005594.

Mégnin, C., Bunge, H.-P., Romanowicz, B., Richards, M.A., 1997. Imaging 3-D spherical convection models, what can seismic tomography tell us about mantle dynamics? Geophys. Res. Lett. 24 (11), 1299–1303.

Morgan, W.J., 1984. Hotspot tracks and the opening of the Atlantic and Indian Oceans. In: Emiliani, C. (Ed.), The Oceanic Lithosphere. : The Sea, Vol. 7. Wiley, New York, pp. 443–487.

Müller, R.D., Royer, J.-Y., Lawver, L.A., 1993. Revised plate motions relative to the hotspots from combined Atlantic and Indian Ocean hotspot tracks. Geology 21, 275–278.

Müller, R.D., Royer, J.-Y., Lawver, L.A., 1994. Revised plate motions relative to the hotspots from combined Atlantic and Indian Ocean Hotspot tracks, Reply. Geology 22, 277–278 1994.

Müller, R.D., Sdrolias, M., Gaina, C., Roest, W.R., 2008. Age, spreading rates and spreading asymmetry of the world's ocean crust. Geochem. Geophys. Geosyst. 9, Q04006. doi:10.1029/2007GC001743.

Norton, I., 1996. The history of global plate motions. Geophys. Monogr. 121, 339–357.

O'Neill, C., Müller, R.D., Steinberger, B., 2005. On the uncertainties in hot spot reconstructions and the significance of moving hot spot reference frames. Geochem. Geophys. Geosyst. 6, Q04003. doi:10.1029/2004GC000784.

Oeser, J., Bunge, H.-P., Mohr, M., 2006. Cluster design in the Earth Sciences Tethys. High Performance Computing and Communications, Proceedings: Lecture Notes in Computer Science: 2nd International Conference on High Performance Computing and Communications (HPCC 2006), Sept 13–15, 2006, Munich, Germany, vol. 4208, pp. 31–40.

Prévot, M., Mattern, E., Camps, P., Daignières, M., 2000. Evidence for a 20° tilting of the Earth's rotation axis 110 million years ago. Earth Planet. Sci. Lett. 179, 517–528. doi:10.1016/ S0012-821X(00)00129.

Rao, G.V.S.P., Rao, J.M., 1996. Palaeomagnetism of the Rajmahal traps of India, implication to the reversal in the Cretaceous Normal Superchron. J. Geomagnet. Geoelect. 48, 993–1000.

Ritsema, J., van Heijst, H.J., Woodhouse, J.H., 1999. Complex shear wave velocity structure imaged beneath Africa and Iceland. Science 286, 1925–1928.

Ritsema, J., van Heijst, H.J., Woodhouse, J.H., 2004. Global transition zone tomography. J. Geophys. Res. 109, B02302. doi:10.1029/2003JB002610.

Ritsema, J., McNamara, A.K., Bull, A.L., 2007. Tomographic filtering of geodynamic models: implications for model interpretation and large-scale mantle structure. J. Geophys. Res. 112, B01303. doi:10.1029/2006JB004566.

Schaber, K., Bunge, H.-P., Schuberth, B.S.A., Malservisi, R., Horbach, A., 2009. Stability of the rotation axis in high-resolution mantle circulation models: weak polar wander despite strong core heating. Geochem. Geophys. Geosyst. 10, Q11W04. doi:10.1029/2009GC002541.

Schuberth, B.S.A., Bunge, H.-P., Steinle-Neumann, G., Moder, C., Oeser, J., 2009a. Thermal versus elastic heterogeneity in high-resolution mantle circulation models with pyrolite composition: high plume excess temperatures in the lowermost mantle. Geochem. Geophys. Geosyst. 10, Q01W01. doi:10.1029/2008GC002235.

Schuberth, B.S.A., Bunge, H.-P., Ritsema, J., 2009b. Tomographic filtering of high-resolution mantle circulation models: can seismic heterogeneity be explained by temperature alone? Geochem. Geophys. Geosyst. 10, Q05W03. doi:10.1029/2009GC002401.

Seton, M., Müller, R.D., Zahirovic, S., Gaina, C., Torsvik, T., Shephard, G., Talsma, A., Gurnis, M., and Turner M., in review. Global continental and ocean basin reconstructions since 200 Ma. Earth Science Reviews.

Steinberger, B., 2000. Slabs in the lower mantle — results of dynamic modelling compared with tomographic images and the geoid. Phys. Earth Planet. Int. 118, 241–257.

Steinberger, B., Torsvik, T., 2008. Absolute plate motions and true polar wander in the absence of hotspot tracks. Nature 452, 620–624. doi:10.1038/nature06842.

Steinberger, B., Torsvik, T.H., 2010. Toward an explanation for the present and past locations of the poles. Geochem. Geophys. Geosyst. Q06W06. doi:10.1029/2009GC002889.

Stixrude, L., Lithgow-Bertelloni, C., 2005. Thermodynamics of mantle minerals — I. physical properties. Geophys. J. Int. 162, 610–632. doi:10.1111/j.1365-246X.2005.02642.x.

Stixrude, L., Lithgow-Bertelloni, C., 2007. Influence of phase transformations on lateral heterogeneity and dynamics in Earth's mantle. Earth Planet. Sci. Lett. 263, 45–55. doi:10.1016/j.epsl.2007.08.027.

Styles, E., Davies, D.R., Goes, S., 2011. Mapping spherical seismic into physical structure: biases from 3-D phase-transition and thermal boundary-layer heterogeneity. Geophys. J. Int. 184, 1371–1378.

Tarduno, J., Bunge, H.-P., Sleep, N., Hansen, U., 2009. The bent Hawaiian-emperor hotspot track: inheriting the mantle wind. Science 324, 50–53.

Tolstikhin, I., Hoffmann, A.W., 2005. Early crust on top of the Earth's core. Phys. Earth Planet. Int. 148, 109–130.

Torsvik, T., Müller, R., van der Voo, R., Steinberger, B., Gaina, C., 2008. Global plate motion frames: toward a unified model. Rev. Geophys. 46, 1–44. doi:10.1029/2007RG000227.

Torsvik, T.H., Steinberger, B., Gurnis, M., Gaina, C., 2010. Plate tectonics and net lithosphere rotation over the past 150 Myr. Earth Planet. Sci. Lett. 291, 106–112.

van der Meer, D.G., Spakman, W., van Hinsbergen, D.J.J., Amaru, M.L., Torsvik, T.H., 2010. Towards absolute plate motions constrained by lower-mantle slab remnants. Nat. Geosci. 3, 36–40.

Van Fossen, M.C., Kent, D.V., 1992. Paleomagnetism of 122 Ma plutons in New England and the Mid-Cretaceous paleomagnetic field in North America: true polar wander or large-scale differential mantle motion? J. Geophys. Res. 97, 19,651–19,661.

Wessel, P., Kroenke, L.W., 2008. Pacific absolute plate motions since 145 Ma. J. Geophys. Res. 113 (B06101). doi:10.1029/2007JB005499.

Wessel, P., Harada, Y., Kroenke, L.W., 2006. Toward a self-consistent, high-resolution absolute plate motion model for the Pacific. Geochem. Geophys. Geosyst. 7, Q03L12. doi:10.1029/2005GC001000.

Wilson, J.T., 1963. A possible origin of the Hawaiian Islands. Can. J. Phys. 41, 863–870.